RESEARCH ARTICLE

Medinformatics 2025, Vol. 00(00) 1–14

DOI: 10.47852/bonviewMEDIN52025991



Computational Genomic Variations of GRIN2B Associated with Autism Spectrum Disorders: An *In Silico* Approach

Srushti S. Chavadapur¹ and Nallur B. Ramachandra^{1,*}

¹Department of Studies in Genetics and Genomics, University of Mysore, India

Abstract: Genomic variations in GRIN2B have been linked to various neurodevelopmental disorders including autism spectrum disorders (ASD). Unraveling variations that modify the protein's structure and function is essential for the possible treatment of diseases. Here, we report *in silico* analysis of all the ASD-specific genomic variations found in GRIN2B and their roles in the pathogenesis of ASD. GRIN2B variations were collected through databases and text mining. These variants were predicted for pathogenicity scores using Varsome tools, and protein domains were predicted using InterPro. Mapping of these variants was done manually. A structural and functional analysis of GRIN2B was also conducted. The GRIN2B gene has 14 exons, and the transcripts expressed in the brain encode 1484 amino acids. Among the 379 ASD-specific variants collected, 54 had a pathogenicity score >60%. Of these, four variants, p.G459E, p.G459R, p.E657G, and p.G820R, showed pathogenic scores >80%. The homology modeling built for these variants indicated that the variants can disrupt the GRIN2B protein. The network analysis revealed that the GRIN2B protein is biologically connected. Among all the variations, 13 variations are key to consider for possible diagnostic and therapeutic approaches. Hence, the *in silico* analysis reveals that the most deleterious variations impair the function of GRIN2B, resulting in altered Central Nervous System development that contributes to ASD.

Keywords: autism spectrum disorder, genomic variations, deleterious variations, secondary structure, receptor, neurodevelopmental disorder

1. Introduction

GRIN2B is a member of the family of seven genes: GRIN1, GRIN2A, GRIN2B, GRIN2C, GRIN2D, GRIN3A, and GRIN3B. These genes encode proteins that together form a receptor responsible for sending chemical messages between neurons in the brain. These proteins are components of N-methyl-D-aspartate (NMDA) receptor complexes that function as heterotetrameric, ligand-gated ion channels with high calcium permeability and voltage-dependent sensitivity to magnesium. Channel activation requires binding of the neurotransmitter glutamate to the epsilon subunit, glycine binding to the zeta subunit, and membrane depolarization to eliminate channel inhibition by Mg²⁺ [1]. Disruption of the GRIN2B receptor protein causes abnormal synaptogenesis, leading to an imbalance between excitatory and inhibitory currents that contribute to the pathogenesis of various neurodevelopmental diseases, particularly autism spectrum disorders (ASD) [2]. However, the information is limited on how improper NMDA receptor activation compromises typical brain growth and development or why excessive activity manifests in neurological complications in people with GRIN2B-related neurodevelopmental disorders.

GRIN2B and its genetic variations are linked to various neurodevelopmental disorders, including ASD [3]. GRIN2B is a highly confident score 1 gene reported in the SFARI database,

indicating its association with ASD [4]. Our earlier studies on ASD, employing various approaches such as global primary hits, global exome sequencing, and homozygosity mapping, identified an association between GRIN2B and ASD. Identifying diseasecausing genomic variations is essential in contemporary genomic research. Next Generation Sequencing technologies have generated vast amounts of data, linking patient genomic variability to brain disorder phenotypes. Sharma et al. [5] studied the association between AT2R and its variants and several diseases, particularly hypertension, to develop AT2R as a potential drug target. They reported that the association of Single Nucleotide Polymorphism (SNPs) (A1675G/G/A1332 G) with alternate splicing of AT2R mRNA, A1332G variants with the shortening of the AT2R mRNA, specifically SNP(C4599A) in females and SNP(T1334C) in males, was associated with the diseases. Further, computational investigation of the impact of potential AT2R polymorphism on small molecule binding was also reported [6]. Such studies with more sophisticated computational approaches are beneficial in detecting high-risk variations. Therefore, characterizing the pharmacological of GRIN2B variant receptors could provide opportunities for translational therapeutic strategies for ASD [7]. The deleterious variations in GRIN2B and their interactions may play a crucial role in the pathogenesis of ASD. Bioinformatics studies on the functional effects of structural variations of GRIN2B on ASD have not yet been addressed, despite various studies demonstrating a link between variations in this gene and various diseases. Here, we report all the ASD-specific genomic

^{*}Corresponding author: Nallur B. Ramachandra, Department of Studies in Genetics and Genomics, University of Mysore, India. Email: ramachandra@genetics.uni-mysore.ac.in

[©] The Author(s) 2025. Published by BON VIEW PUBLISHING PTE. LTD. This is an open access article under the CC BY License (https://creativecommons.org/licenses/by/4.0/).

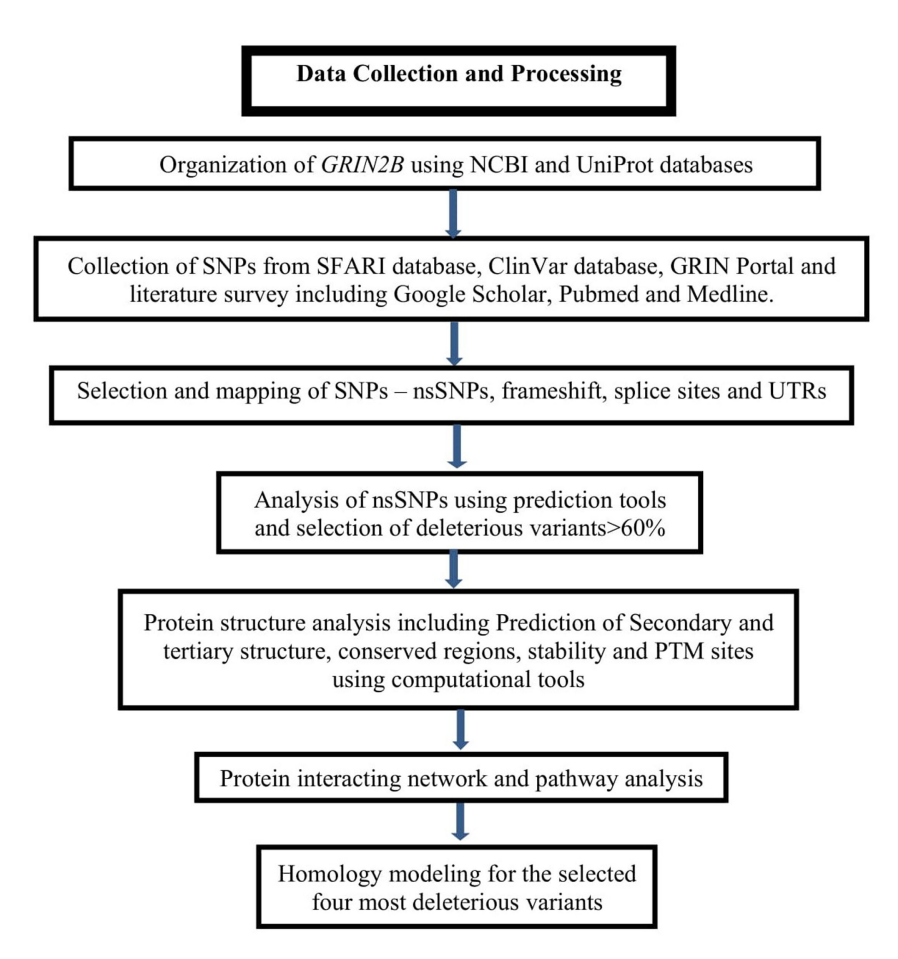


Figure 1. Schematic representation of the workflow of the present study

variations found in GRIN2B, including their pathogenic effects, functional impacts, conservation analyses, post-translational alterations driving residues, and the dynamic behaviors of deleterious variations on protein models.

2. Materials and Methods

2.1. GRIN2B sequence information retrieval

Nucleotide sequence of GRIN2B [8] in FASTA format was collected from the NCBI (http://www.ncbi.nlm.nih.gov accessed in March 2024). The protein sequence of GRIN2B [9], downloaded from UniProt (https://www.uniprot.org/, accessed in March 2024), was used in the present study.

2.2. Data collection and processing

ASD subject-specific genomic variations of GRIN2B were collected from the SFARI repository [4], ClinVar [10], GRIN Portal database [11], and text mining using three search tools. The detailed steps for data collection and processing are provided in Figure 1. ClinVar is a freely accessible, public archive of reports on human variations classified by disease and drug response, along with supporting evidence [10]. The GRIN Portal is a coalition of investigators seeking to aggregate and harmonize data generated to study GRIN-related disorders, making summary data interactively accessible to the broader scientific community while providing educational resources for all [10].

For text mining, search tools Google Scholar, Medline, and PubMed were utilized, employing MeSH search keywords such as GRIN2B, neurodevelopmental disorder, and ASD. All these data were accessed on March 28, 2024. The detailed steps followed in text mining are provided in Figure 2.

Variants were collected and processed according to stringent exclusion and inclusion criteria. The study included all nonsynonymous, truncating, 3', and 5' untranslated regions variants. The study excluded all synonymous and intronic variants, except for splice site variants. The amino acid residues of GRIN2B were sub-grouped into their domains, motifs, and loop regions. The position and number of amino acid variations within each sub-region were determined. All the truncating variants, that is, frameshift deletion/insertion and stop gain or loss variants, were regarded as loss-of-function variants. Further, all the nonsynonymous variants were subjected to pathogenicity prediction analysis to identify the most deleterious variants.

2.3. Mapping of GRIN2B variants

Varsome is an online server used to predict deleterious variants (https://varsome.com/, accessed in March 2024) [12]. For predicting protein domains, InterPro (https://www.ebi.ac.uk/interpro/ accessed in March 2024) was utilized. Among all the variations collected from different databases and text mining, only nonsynonymous variants were further analyzed by using a total of 22 different tools from Varsome, including BayesDeladdAF, BayesDelnoAF, Meta SVM, EVE, LRT, MetaRNN [13], M-CAP [12], MetaLR and Mutation Accessor [13], SIFT4G [14], DANN [15], DEOGEN2 [16], BLOSUM [17], EIGEN and EIGENPC [18], FATHMM-MKL [19], FATHMM-XF [20], MVP [21], PrimateAI [22], MutPred [23], Mutation taster [24], and LIST-S2 [25]. These tools were

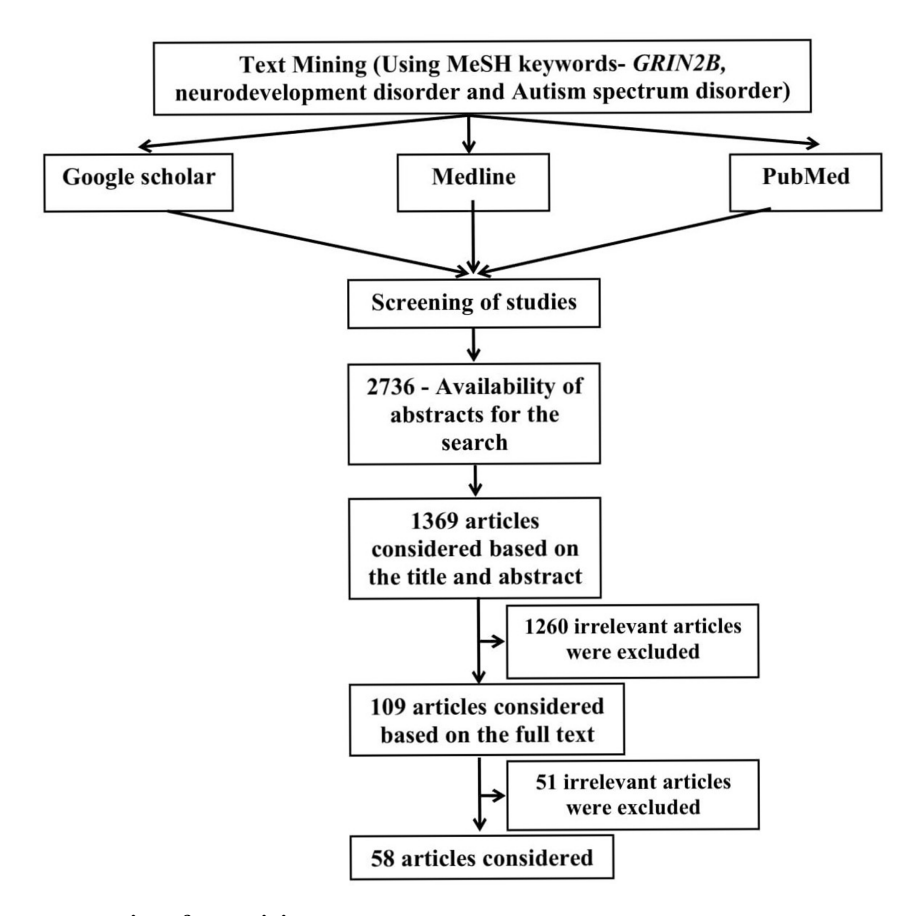


Figure 2. Schematic representation of text mining

used to determine the pathogenicity status of the variants, including pathogenic, strongly pathogenic, pathogenic supporting, and moderately pathogenic. Based on this information, we calculated the pathogenicity percentage and selected the variants with the highest percentage, indicating pathogenicity. A nonsynonymous variant was considered as confirmed 'deleterious (D)' only if >60% of tools predicted it as a damaging variant. All deleterious variations were predicted within all domains, motifs, loops, and regions outside them to identify the most mutationally sensitive regions of GRIN2B. All the deleterious variants predicted were manually mapped on GRIN2B.

2.4. Study of protein structure, function, and stability

The secondary structure was predicted based on sequence information from the PSSpred algorithm [26] for GRIN2B, which combines seven neural network predictors from different parameters and PSI-BLAST [27] profile data. For 3D protein structure prediction and structure-based function annotation, a hierarchical approach called I-TASSER was used [28].

2.5. Sequence conservation analysis

To analyze protein conservation and predict protein target area high-throughput functions [29], ConSurf, an online software (http://ConSurf.tau.ac.il/ accessed on March 14, 2024), was used. This tool takes FASTA protein sequences as input. The conservation analysis was shown on a scale of 1–9 for each relevant protein residue. On the scale, 1–3 represent variable regions, 4–6 represent the average region, and 7–9 represent highly preserved regions [29].

2.6. Prediction of phosphorylation sites (PTMs)

Various amino acid alterations occur as post-translational modifications (PTMs), including methylation, phosphorylation, acetylation, and ubiquitination, resulting in a diverse spectrum of proteins. Consequently, projecting PTM data assists in assessing the influence of polymorphisms on disease association or pathogenicity. MuSiteDeep – a deep-learning-based webserver for protein PTM site prediction and visualization – was used [30]. NetPhos 3.1 [31] server predicts phosphorylation sites using ensembles of neural networks. This tool was used to identify phosphorylation sites on serine (S) and tyrosine (Y) residues.

2.7. Prediction of normal and variant protein structures

The Swiss model is an online server used to build the homologous model of the query protein sequences for the selected variants [32]. The structural stability of the normal and variant proteins was assessed using structural analysis. Here, sequence-based homology modeling was done for both normal and variant proteins, and the best model was selected as the target based on the highest sequence identity of >50%. Discovery Studio was used to correct the nomenclature of atoms and model side chains [33]. The SAVES server was used to validate the protein models (http://servicesn.mbi.ucla.edu/SAVES, accessed on June 10, 2024).

2.8. Study of protein-protein interaction (PPI)

The PPI network of GRIN2B was constructed using STRING (https://string-db.org/ accessed on June 25, 2024 [34]).

Table 1	The	detailed	list of	GRIN2B	evons	and	intron	Sizes
Table 1.	1110	uctancu	HSt OI	UIMINAD	CAUIIS	anu	шичи	SIZCS

Sl. no.	Exons of GR	IN2B	Introns of	GRIN2B
	Exon ID	Length (bp)	Intron number	Length (bp)
1	ENSE00003903818	261	Intron 1	985
2	ENSE00003770327	429	Intron 2	113,701
3	ENSE00000993733	429	Intron 3	111,882
4	ENSE00000993731	599	Intron 4	77,457
5	ENSE00000993725	115	Intron 5	59,087
6	ENSE00000993720	203	Intron 6	790
7	ENSE00000993722	172	Intron 7	225
8	ENSE00001667846	154	Intron 8	3,263
9	ENSE00000993729	126	Intron 9	2,892
10	ENSE00000993719	230	Intron 10	36,638
11	ENSE00000993723	161	Intron 11	1,786
12	ENSE00004022628	188	Intron 12	2,566
13	ENSE00000993715	239	Intron 13	2,385
14	ENSE00004022629	27,303		

GRIN2B was used as input, with *Homo sapiens* as the organism of interest. The STRING database incorporates information from various sources, including experimental data, computer prediction techniques, and open text collections. Using various functional categorization systems, including GO, Pfam, and KEGG, the site also highlights functional enrichments in user-provided lists of proteins.

3. Results

3.1. Organization of GRIN2B

The human GRIN2B spans 544,060 bps and is located on the reverse strand of chromosome 12p13.1, from 13437942 to 13982002 bp (https://asia.ensembl.org/Homo_sapiens/Gene/Summa ry?g=ENSG00000273079;r=12:13437942-13982002 accessed on July 17, 2025). This gene produces ten transcripts, among which the transcript with ID ENST00000609686.4 (GRIN2B), expressed in the brain (https://gtexportal.org/home/gene/GRIN2B#gene-transcript-bro wser-block accessed on July 17, 2025), contains 14 exons on the reverse strand and plays a vital role in ASD [34]. ENST00000609686.4/CCDS8662.1/NM_000834.5 are the canonical reference for GRIN2B in most genomic analyses to ensure consistency across Ensembl, CCDS, and RefSeq annotations [35]. This transcript, with 30609bp, codes for 1484 amino acids, as shown in Table 1.

3.2. Types of variations of GRIN2B and their mapping

A comprehensive workflow for data collection and processing on GRIN2B is presented in Figure 1. A systematic literature search of 2,736 articles, published from 2000 to 2024, was conducted using text mining. Out of these, duplicated articles were removed, and 1369 articles without duplicates were eligible for the studies. After reviewing the titles and abstracts, 1260 articles that were not relevant were excluded. Of the remaining 109 articles, 51 were excluded after reviewing the full text based on insufficient firm conclusions. Finally, 58 articles were included in this systematic review, as detailed in Figure 2. A total of 379 ASD-specific variants were collected from the SFARI, ClinVar, and GRIN portal

databases, as well as text mining data. This includes 282 nonsynonymous variants, 17 synonymous variants, 19 frameshift variants, 64 intron variants, and 10 variants from the 3' UTR. After removing the overlapping variants, a total of 153 variants, namely, 117 nonsynonymous variants, 7 from splice sites, 19 frameshift variants, and 10 variants from the 3' UTR, were selected for further analysis. The list of 153 ASD-specific variants, including location, position information, mutation type, and specific reference sources, is provided in Supplementary Table 1.

For GRIN2B, among the 14 exons, 12 (exons 3–14) exhibit both nucleotide and amino acid variations. From exon 6 to exon 13, variations were repeatedly found in different samples. Figure 3(A) illustrates the mapping of 153 variants of GRIN2B based on the Varsome tool. According to the mapping, exons 10, 13, and 14 had the highest number (>20) of variants, exons 8 and 11 had a medium number of variants (>10), and exons 3, 4, 5, 6, 7, 9, and 12 had the lowest number of variants (<10). Our findings revealed three frameshift variants, including insertions, deletions, and duplications, found in exons 3, 4, 9, 11, 13, and 14. Among these exons, exon 13 had the highest number (7) of frameshift variants, including three deletions (c.2384 2391del, c.2555delC, and c.2594delC), three duplications (c.2409_2419dup, c.2479dupG, and c.2590_2593dup), and one insertion (c.2394_2395ins). Exon 11 had only one variant, that is, duplication (c.2208dupC). The exon 3 had one deletion (c.13delC), one duplication (c.99dupC), and two insertions (c.23_24insC and c.91_92insC), exon 4 had three deletions (c.735delG, c.803_804delTG, and c.996delG), exon 9 had one deletion (c.1711delC), and exon 14 had three deletions (c.2825del, c.2862_2863delCA, and c.3937_3940delCTTC). We identified seven splice site variants in the 1, 4, 9, 10, 11, and 12 introns. Among these introns, only intron 10 had two splice sites (c.2010+1G>C and c.2011-5_2011-4del). The remaining introns had only single splice sites such as intron 3 (c.411+1G>A), intron 4 (c.1010+1G>A), intron 9 (c.1780+1G>A), intron 11 (c.2172-2A>A), and intron 12 (c.2360-2A>G). The 10 variants from the 3'UTR region included c.4615C>T, c.5072T>G, c.5806A>C, c.5988T>C, c.6509T>C, c.9215C>T, c.9825A>G, c.15141C>G, c.17075G>C, and c.24377C>T.

All 117 nonsynonymous variants with amino acid changes were mapped on GRIN2B, from exons 3 to 14, as shown in Figure 3(B). Exon 14 had the maximum number of nonsynonymous variants, and

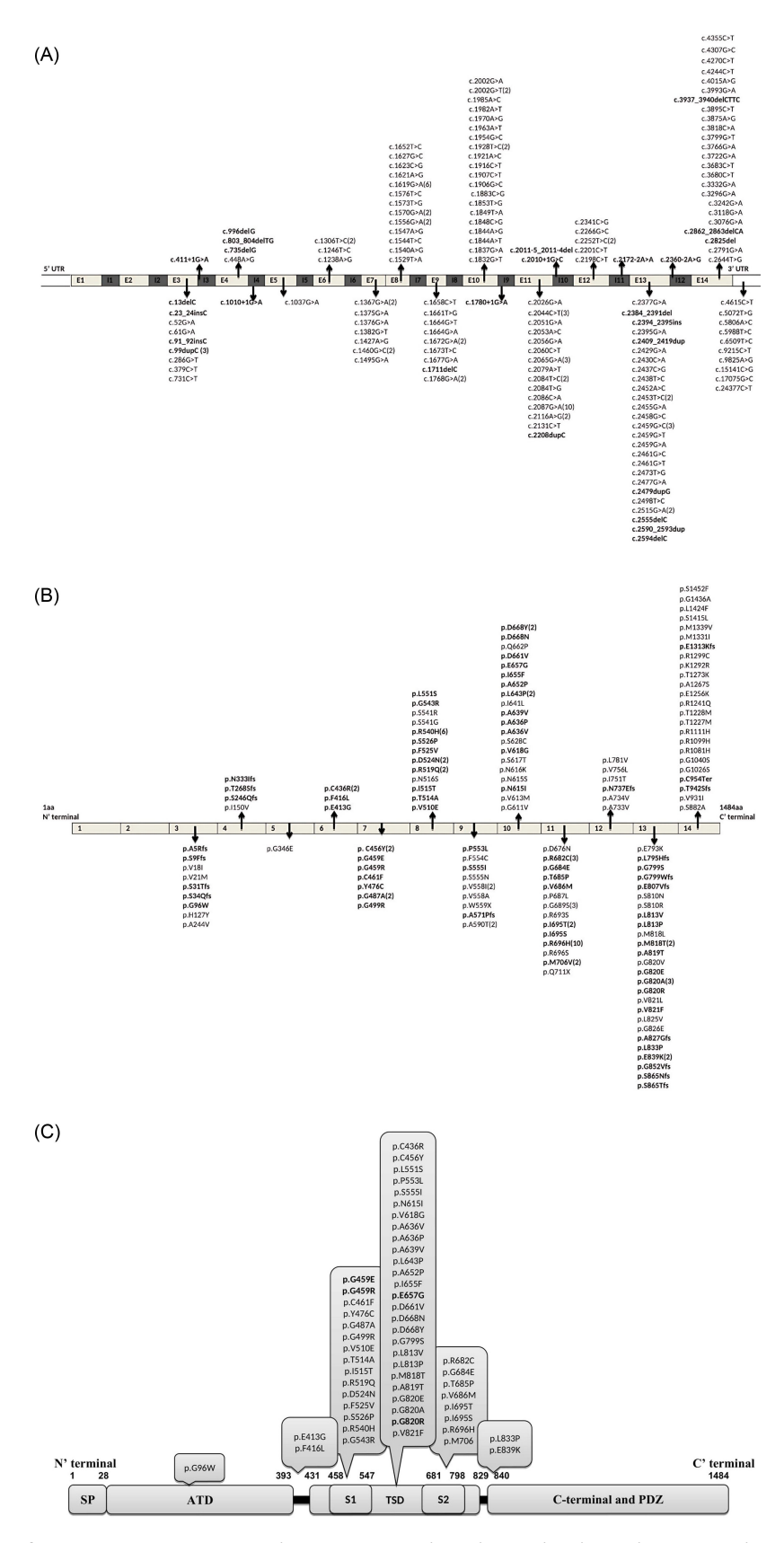


Figure 3. (A) Mapping of all the nonsynonymous variants on the exonic region, splice site variants on the intronic region, and 3' UTR variants on the 3' UTR region of GRIN2B. Variants highlighted with bold letters are frameshift and splice site variants. (B) Mapping of amino acid changes in GRIN2B on the exon regions. Variants highlighted in bold letters are frameshift variants. (C) Predicted domains of GRIN2B. SP, signal peptide; ATD, amino-terminal domain; S1 and S2, the ligand-binding domains; TSD, re-entrant pore-forming and transmembrane spanning domains (pore); PDZ, C-terminus PDZ domain-binding motif. The four most deleterious variants were highlighted in bold letters.

exons 1 and 2 showed no variants. Some variants were observed repeatedly on exons 6–13, except for exon 12. All 19 frameshift variants, including insertions, deletions, and duplications, were also mapped on GRIN2B in exons 3, 4, 9, 11, 13, and 14 and highlighted in Figure 3(B). Furthermore, all 117 nonsynonymous variants were analyzed and categorized into five types based on their level of pathogenicity, specifically 0–20%, 21–40%, 41–60%, 61–80%, and 81–100%. The prediction tool revealed that the 18 variants fell within the 0–20% range, 17 variants fell within the 21–40% range, 28 variants fell within the 41–60% range, 50 variants fell within the 61–80% range, and four variants fell within the 81–100% range. Among them, 54 variants had a pathogenicity score >60%. All these 54 variants were highlighted in bold in Figure 3(B) and selected for further analysis.

The exons and the variants with the pathogenicity score >60% are as follows: exon 3 with one variant (p.G96W), exon 6 with three variants (p.E413G, p.F416L and p.C436R), exon 7 with seven variants (p. C456Y, p.G459E, p.G459R, p.C461F, p.Y476C, p.G487A and p.G499R), exon 8 with 10 variants (p.V510E, p.T514A, p.I515T, p.R519Q, p.D524N, p.F525V, p.S526P, p.R540H, p.G543R, and p.L551S), exon 9 with two variants (p.P553L and p.S555I), exon 10 with 12 variants (p.N615I, p.V618G, p.A636V, p.A636P, p.A639V, p.L643P, p.A652P, p.I655F, p.E657G, p.D661V, p.D668N, and p.D668Y), exon 11 with eight variants (p.R682C, p.G684E, p.T685P, p.V686M, p.I695T, p.I695S, p.R696H, and p.M706V), and exon 13 with 11 variants (p.G799S, p.L813V, p.L813P, p.M818T, p.A819T, p.G820E, p.G820A, p.G820R, p.V821F, p.L833P, and p.E839K). Exons 4, 5, 12, and 14 showed no variants with a pathogenicity score >60%. Among all the exons, all variants located on exons six and seven were found to be pathogenic, with a score >60%.

GRIN2B is 1484 amino acids long and includes conserved domains of the NR2B subunit, that is, signal peptide (SP) from residues 1-28, amino-terminal domain (ATD) from 28-393 that is involved in receptor assembly, S1 from 458-547, S2 from 681-798 that forms the ligand-binding domain, re-entrant pore-forming and transmembrane spanning domains (TSD) from 431–829, and the C-terminus PDZ domain-binding motif (PDZ) from 840-1484 residues, as illustrated in Figure 3(C). All 54 deleterious variants with a pathogenic score >60% were mapped to different domain regions of GRIN2B, as detailed in Table 2. Among these, most pathogenic variants were found in TSD, S1, and S2. Only the variant p.G96W was identified in the ATD domain, suggesting that it is involved in receptor assembly, whereas the PDZ domain did not exhibit any variants. Among all the 54 variants, the four variants, p.G459E, p.G459R, p.E657G, and p.G820R, showed pathogenic scores >80% and were selected for further analysis. The variants p.G459E and p.G459R were found on the S1 domain, which is involved in the ligand-binding process. The other two variants, p.E657G and p.G820R, were found on the TSD throughout, which is involved in the re-entrant pore-forming and transmembrane spanning process.

3.3. GRIN2B protein

The secondary structure of GRIN2B is predicted to consist of 37 alpha helices (H), 27 beta sheets (S), and 1420 coils (C). The analysis revealed that both helices and strands are shaped by hydrogen bonding between the carbonyl 'O of one amino acid and the amino H of another. These hydrogen atoms constitute nearly half of the atoms in a protein. They mediate hydrogen bonds and participate in noncovalent interactions including electrostatic and van der Waals forces. Prediction revealed that among all the 54

deleterious variants, 23 were alpha helices, 9 were beta sheets, and 22 were coils, indicating that more alpha helices could tolerate more variations than beta sheets. I-TASSER predicted models with a C-score of >-1.5 possessed a correct topology. The TM-score ranges from 0 to 1, with higher values showing better structural models. The present study revealed that the first model had a better structure, with a C-score of -2.73, a TM-score of 0.41 \pm 0.13, and an RMSD of 17.1 \pm 2.7 Å, which was used for further analysis.

Solvent accessibility was predicted, and the results showed that solvent accessibility at the bottom was presented in 10 levels, from buried (0) to highly exposed (9). This indicates that most amino acids with the selected 54 variants were moderately exposed to the solvent. Most N- and C-terminal regions were predicted to have positive normalized B-factors, indicating that these regions are structurally more flexible than other regions.

3.4. Conserved residues of GRIN2B

The ConSurf server predicted the conserved behavior on a scale of 1–9, with color codes ranging from blue to purple, where blue indicates variability and purple indicates a highly conserved location. On the scale, 1–3 represented variable, 4–6 represented the average, and 7–9 represented highly conserved regions. The results of the ConSurf prediction revealed that all 54 selected deleterious variants were found to be conserved, especially in the region of the TSD, highlighted in the red-colored box and shown in Figure 4.

3.5. Phosphorylation sites on GRIN2B

The MusiteDeep and NetPhos 3.1 servers predicted PTMs associated with 113 nonsynonymous variants identified in the present study, using the protein sequence. These findings were obtained in .csv format, and all nonsynonymous variants were evaluated. Among them, 43 were shown to contribute to phosphorylation, including 41 phosphothreonine, and only two were phosphoserine. The descriptions of the 43 nonsynonymous variants involved in phosphorylation are provided in Table 3. Using ensemble neural networks, the NetPhos 3.1 server predicted serine, threonine, or tyrosine phosphorylation sites in the GRIN2B protein. Generic and kinase-specific predictions yielded scores >0.5, indicating optimistic predictions. Predictions were made using the selected prediction score of >0.5 for the 17 kinases, including ATM, CKI, CKII, CaMII, DNAPK, EGFR, GSK3, INSR, PKA, PKB, PKC, PKG, RSK, SRC, cdc2, cdk5, and p38 MAPK. The results revealed that all 43 predicted PTM sites with a score >0.5 were accurate predictions.

3.6. Comparison of normal and variant protein structures of GRIN2B

The findings showed that variations in GRIN2B at p.G459E, p.G459R, p.E657G, and p.G820R induced pathogenicity with a score >80%. The variant p.G459R had a pathogenicity score of 86.36%, while the remaining three variants had a score of 81.81%. These four highly conserved variants were used to determine the changes in protein structure they produce. Using the Swiss model, we obtained five templates for each variant, with the model exhibiting 98.99% sequence identity. Sequence coverage of >50% was selected for each variant. SAVES gives the result with the quality factor score for each variant, such as 91.14% for p.Gly459Glu, 94.86% for p.Gly459Arg, 94.58% for p.Glu657Gly,

Table 2. The detailed list of all 54 deleterious variants of GRIN2B with a pathogenicity score >60%

Allele change	Residue change	Pathogenicity in %	Domain	Conservation level	Exon number
c.1970A>G	p.E657G	81.81	TSD	Conserved	10
c.1376G>A	p.G459E	81.81	S1	Conserved	7
c.2002G>T	p.D668Y	77.27	TSD	Highly Conserved	10
c.2044C>T	p.R682C	77.27	S2	Highly Conserved	11
c.1427A>G	p.Y476C	77.27	S1	Highly Conserved	7
c.2515G>A	p.E839K	77.27	No domain	Highly Conserved	13
c.1658C>T	p.P553L	77.27	TSD	Highly Conserved	9
c.1664G>T	p.S555I	77.27	TSD	Highly Conserved	9
c.1963A>T	p.I655F	77.27	TSD	Highly Conserved	10
c.2459G>T	p.G820V	77.27	TSD	Highly Conserved	13
c.2053A>C	p.T685P	77.27	S2	Highly Conserved	11
c.2459G>A	p.G820E	77.27	TSD	Highly Conserved	13
c.1573T>G	p.F525V	77.27	S1	Highly Conserved	8
c.1619G>A	p.R540H	72.72	S1	Highly Conserved	8
c.2056G>A	p.V686M	72.72	S2	Highly Conserved	11
c.1844A>T	p.N615I	72.72	TSD	Highly Conserved	10
c.1238A>G	p.E413G	72.72	No domain	Highly Conserved	6
c.2084T>C	1	72.72	S2	Highly Conserved	11
c.2459G>C	p.I695T	72.72	TSD		13
c.1906G>C	p.G820A	72.72	TSD	Highly Conserved	
	p.A636P			Highly Conserved	10
c.1460G>C	p.G487A	72.72	S1	Highly Conserved	7
c.2438T>C	p.L813P	72.72	TSD	Highly Conserved	13
c.1928T>C	p.L643P	72.72	TSD	Highly Conserved	10
c.1382G>T	p.C461F	72.72	S1	Highly Conserved	7
c.1246T>C	p.F416L	68.18	No domain	Highly Conserved	6
c.286G>T	p.G96W	68.18	ATD	Highly Conserved	3
c.1367G>A	p.C456Y	68.18	TSD	Highly Conserved	7
c.1556G>A	p.R519Q	68.18	S1	Highly Conserved	8
c.1570G>A	p.D524N	68.18	S1	Highly Conserved	8
c.2002G>A	p.D668N	68.18	TSD	Highly Conserved	10
c.1853T>G	p.V618G	68.18	TSD	Highly Conserved	10
c.1306T>C	p.C436R	68.18	TSD	Conserved	6
c.1495G>A	p.G499R	68.18	S1	Highly Conserved	7
c.1907C>T	p.A636V	68.18	TSD	Highly Conserved	10
c.2116A>G	p.M706V	68.18	S2	Conserved	11
c.2455G>A	p.A819T	68.18	TSD	Highly Conserved	13
c.2498T>C	p.L833P	63.63	No domain	Highly Conserved	13
c.2087G>A	p.R696H	63.63	S2	Highly Conserved	11
c.2395G>A	p.G799S	63.63	TSD	Highly Conserved	13
c.1540A>G	p.T514A	63.63	S1	Highly Conserved	8
c.1916C>T	p.A639V	63.63	TSD	Highly Conserved	10
c.2453T>C	p.M818T	63.63	TSD	Highly Conserved	13
c.2437C>G	p.L813V	63.63	TSD	Highly Conserved	13
c.2461G>T	p.V821F	72.72	TSD	Highly Conserved	13
c.1576T>C	p.S526P	68.18	S1	Highly Conserved	8
c.1627G>C	p.G543R		S1		
	•	63.63		Highly Conserved	8
c.1544T>C	p.I515T	72.72 72.73	S1	Highly Conserved	8
c.1982A>T	p.D661V	72.72	TSD	Highly Conserved	10
c.1375G>A	p.G459R	86.36	S1	Highly Conserved	7
c.1652T>C	p.L551S	77.27	TSD	Conserved	8
c.1529T>A	p.V510E	68.18	S1	Highly Conserved	8
c.2051G>A	p.G684E	77.27	S2	Highly Conserved	11
c.2458G>C	p.G820R	81.81	TSD	Highly Conserved	13
c.2084T>G	p.I695S	72.72	S2	Highly Conserved	11
c.1954G>C	p.A652P	77.27	TSD	Highly Conserved	10

and 94.57% for p.Gly820Arg. These predicted values were expressed as the percentage of the protein for which the calculated error value falls below the 95% rejection limit. Good-quality, high-resolution structures generally produce values of 95% or

higher. For lower resolutions (2.5–3A°), the average overall quality factor was around 91%. The present study's findings revealed that variants p.G459R, p.E657G, and p.G820R were high-quality structures with high resolution, whereas p.G459E was

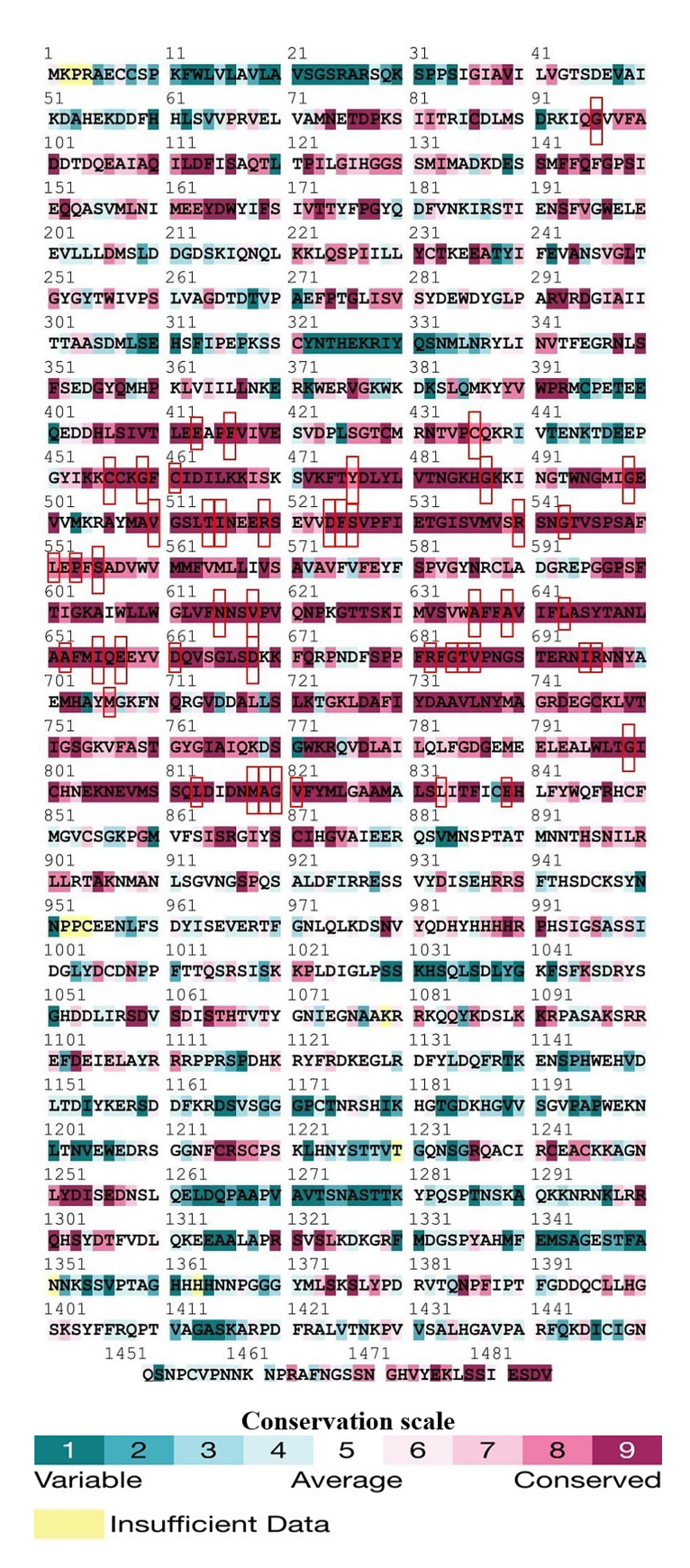


Figure 4. Evolutionary conservation analysis was performed for GRIN2B with the UniProt ID Q13224 in the ConSurf tool. Legends are given on a conservation scale, and all 54 deleterious variants are highlighted in red boxes.

Table 3. Predicted GRIN2B phosphorylation sites

Sl. no.	ID	Position	Residue	PTM site	PTM score (≥0.5)
1	NC_000012.12:c13982134-13537337	31	S	Phosphoserine	0.621
2	NC_000012.12:c13982134-13537337	225	S	Phosphoserine	0.672
3	NC_000012.12:c13982134-13537337	350	S	Phosphoserine	0.723
4	NC_000012.12:c13982134-13537337	678	S	Phosphoserine	0.881
5	NC_000012.12:c13982134-13537337	685	T	Phosphothreonine	0.582
6	NC_000012.12:c13982134-13537337	690	S	Phosphoserine	0.598
7	NC_000012.12:c13982134-13537337	882	S	Phosphoserine	0.649
8	NC_000012.12:c13982134-13537337	886	S	Phosphoserine	0.779
9	NC_000012.12:c13982134-13537337	917	S	Phosphoserine	0.888
10	NC_000012.12:c13982134-13537337	920	S	Phosphoserine	0.728
11	NC_000012.12:c13982134-13537337	929	S	Phosphoserine	0.867
12	NC_000012.12:c13982134-13537337	930	S	Phosphoserine	0.875
13	NC_000012.12:c13982134-13537337	940	S	Phosphoserine	0.713
14	NC_000012.12:c13982134-13537337	993	S	Phosphoserine	0.736
15	NC_000012.12:c13982134-13537337	996	S	Phosphoserine	0.553
16	NC_000012.12:c13982134-13537337	999	S	Phosphoserine	0.542
17	NC_000012.12:c13982134-13537337	1017	S	Phosphoserine	0.503
18	NC_000012.12:c13982134-13537337	1033	S	Phosphoserine	0.561
19	NC_000012.12:c13982134-13537337	1036	S	Phosphoserine	0.565
20	NC_000012.12:c13982134-13537337	1043	S	Phosphoserine	0.654
21	NC_000012.12:c13982134-13537337	1050	S	Phosphoserine	0.723
22	NC_000012.12:c13982134-13537337	1058	S	Phosphoserine	0.693
23	NC_000012.12:c13982134-13537337	1061	S	Phosphoserine	0.649
24	NC_000012.12:c13982134-13537337	1064	S	Phosphoserine	0.56
25	NC_000012.12:c13982134-13537337	1088	S	Phosphoserine	0.768
26	NC_000012.12:c13982134-13537337	1095	S	Phosphoserine	0.627
27	NC_000012.12:c13982134-13537337	1116	S	Phosphoserine	0.861
28	NC_000012.12:c13982134-13537337	1143	S	Phosphoserine	0.825
29	NC_000012.12:c13982134-13537337	1166	S	Phosphoserine	0.792
30	NC_000012.12:c13982134-13537337	1168	S	Phosphoserine	0.616
31	NC_000012.12:c13982134-13537337	1255	S	Phosphoserine	0.755
32	NC_000012.12:c13982134-13537337	1259	S	Phosphoserine	0.827
33	NC_000012.12:c13982134-13537337	1284	S	Phosphoserine	0.879
34	NC_000012.12:c13982134-13537337	1288	S	Phosphoserine	0.532
35	NC_000012.12:c13982134-13537337	1303	S	Phosphoserine	0.91
36	NC_000012.12:c13982134-13537337	1306	T	Phosphothreonine	0.674
37	NC_000012.12:c13982134-13537337	1323	S	Phosphoserine	0.756
38	NC_000012.12.c13982134-13537337 NC_000012.12:c13982134-13537337	1323	S	Phosphoserine	0.714
39	NC_000012.12:c13982134-13537337	1468	S	Phosphoserine	0.634
39 40		1468	S S	Phosphoserine	0.634
40 41	NC_000012.12:c13982134-13537337	1469	S S	Phosphoserine Phosphoserine	0.39 0.725
	NC_000012.12:c13982134-13537337		S S		
42	NC_000012.12:c13982134-13537337	1479		Phosphoserine	0.849
43	NC_000012.12:c13982134-13537337	1482	S	Phosphoserine	0.821

an average structure with low resolution. The finalized structures in 3D orientations are represented in Figure 5.

3.7. Protein-protein interaction (PPI) network

A PPI network was constructed for GRIN2B using the STRING database, yielding a complex network of 10 interactions among 11 nodes. The results revealed that the resultant edges were 51, which is more than the expected number of interactions, indicating that the GRIN2B protein is biologically connected as a group. The statistical data revealed that the average node degree was 9.27, the average local clustering coefficient was 0.943, and the PPI enrichment p-value was <1.0e - 16. The interaction network is presented in Figure 6, which includes network nodes and edges. Only interactions with a confidence score that is more significant than the lowest needed interaction score are involved in the predicted network. More engagement, but with higher false positives, is associated with lower

scores. The confidence score represented the likelihood of a predicted association between two proteins in the metabolic pathway database. The bounds of confidence are as follows: low confidence – 0.15, medium confidence – 0.4, high confidence – 0.7, and highest confidence – 0.9. The STRING database predicted that all the functional partners, such as GRIN2A, GRIN1, GRIN2D, GRIN2C, GRIN3A, DLG4, GRIN3B, DLG3, CAMK2A, and DLG2, were found with a score of 0.99, suggesting that all these partners were highly confident in their interaction with GRIN2B. The data is given in Supplementary Table 1.

4. Discussion

4.1. GRIN2B variations

GRIN2B facilitates calcium-permeable excitatory synaptic transmission between neurons in the brain. Many genomic

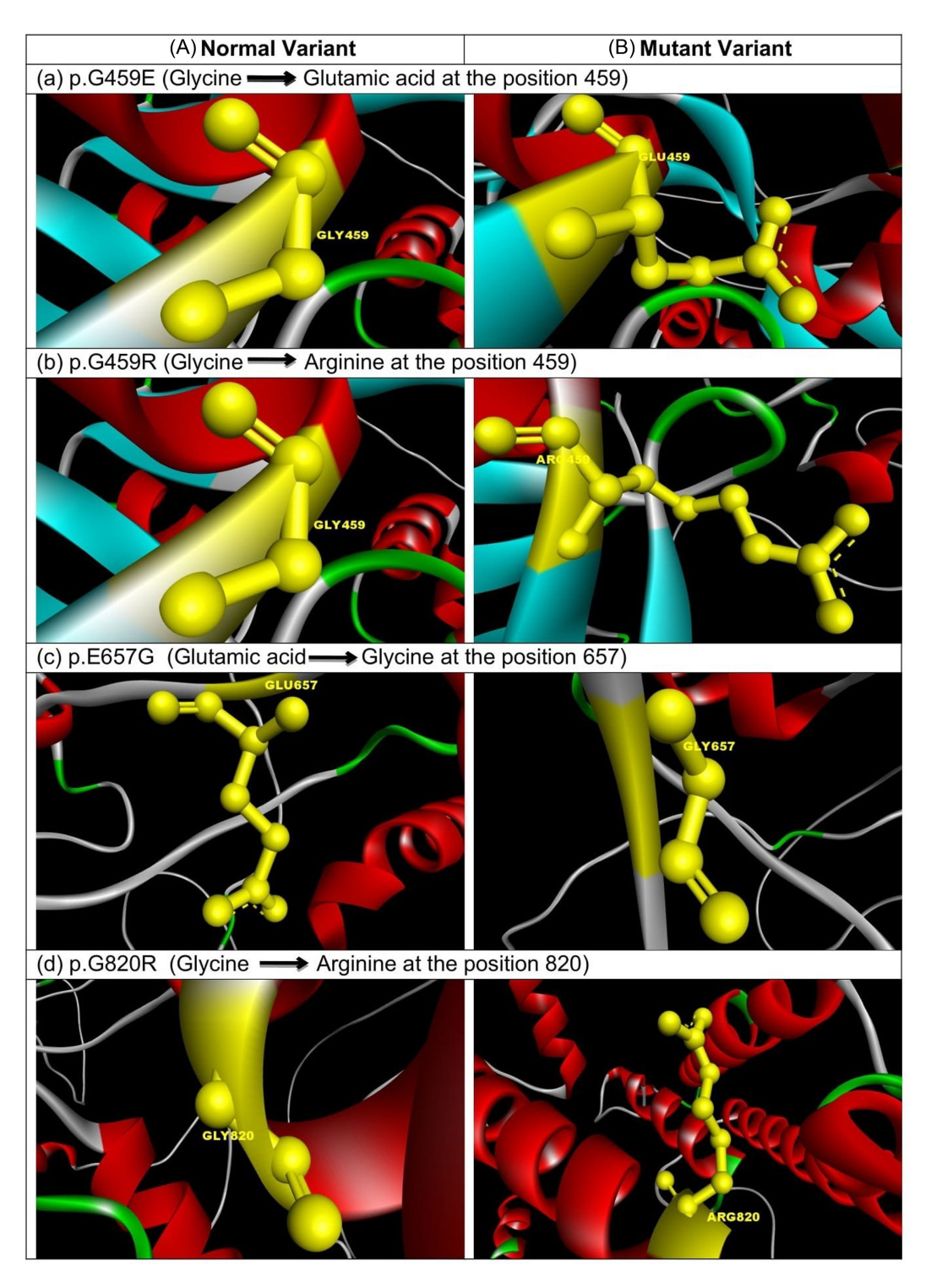


Figure 5. 3D images of four variants are represented with normal amino acid on the left and a mutant on the right. The site of the variant replaced the amino acid with a cavity, which is represented by a ball-and-stick structure at the center in yellow, surrounded by alpha helices and beta sheets.

variations in this gene are reported with their association with neurodevelopmental disorders such as ASD, Attention Deficit/ Hyperactivity Disorder, epilepsy, and schizophrenia [2]. A meta-analysis of a triad family cohort and a case-control cohort from a Chinese population has identified significant associations between multiple common variants and autism risk [36].

The present study involves extracting and analyzing large amounts of raw genomic variation data from text mining and

databases to identify and map the GRIN2B variations associated with ASD comprehensively. Out of the 379 variations found in GRIN2B, not all are relevant for the disease's pathogenicity, as many are random, nonspecific, and silent variations. Of the 117 nonsynonymous variants, 54 had a pathogenicity score >60%, indicating their potential to disrupt protein function. Among all the exons, the nonsynonymous variants found in exons six and seven are pathogenic, highlighting their potential impact on protein

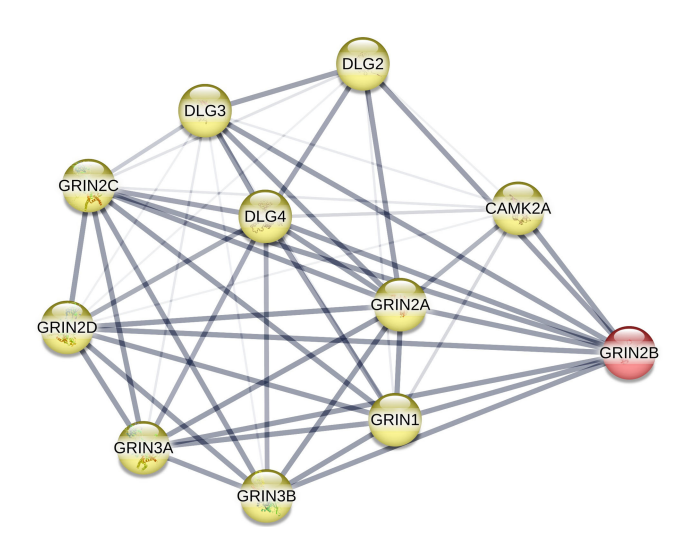


Figure 6. Predicted interaction network around GRIN2B. From a confident perspective, the thicker lines represent a stronger association, while the thinner lines indicate a weaker association. All the proteins that undergo interaction are represented in ball structures known as nodes. The colored node represents the query protein GRIN2B, which corresponds to the first shell of interaction. Other nodes, highlighted in yellow, represent functional partners that exhibit direct interaction with GRIN2B.

function. Additionally, as frameshift variants are considered major causes of disease, the present study identified 19 high-prevalence frameshift variants in exons 3, 4, 13, and 14. Notably, those located in the N-terminal regions posed a greater threat to the gene's functionality than those in the C-terminal regions. Similarly, variations in the splice site of the gene can disrupt RNA splicing, leading to the inclusion of introns or loss of exons, thereby disrupting the protein-coding sequence [37]. All the frameshift and splice site variants lead to premature chain termination of GRIN2B transcripts, which results in haploinsufficiency. Understanding these prevalent variants can significantly enhance the diagnosis and treatment of ASD. The 3' UTR region of the gene is larger and has 10 variants. These variants could potentially influence mRNA localization, stability, and translation, thereby affecting the production of the GRIN2B protein.

ENST00000609686.4 (GRIN2B-201) is the major functional isoform widely expressed in the brain, and includes all key regulatory and channel-targeting domains. It is essential to recognize the isoform diversity of GRIN2B, as alternative splicing generates multiple transcript variants with differences in regulatory regions and protein domains. While the majority of pathogenic variants reported so far occur in exons shared across all major isoforms, some variants may localize to exons that are skipped in minor isoforms. This raises the possibility that the functional and clinical impact of a variant could vary depending on isoform expression patterns, particularly in brain regions or developmental stages where certain isoforms predominate [38]. In the present study, the GRIN2B brain transcript is a full-length isoform without any exon reshuffling, indicating that any deleterious variant disrupts the protein function.

4.2. Effect of variations on protein structure and function

The ligand-binding domain is the clamshell-shaped extracellular domain where glutamate binds. The variations in this domain can

affect agonist affinity, gating efficiency, and kinetics, changing how well ligand binding translates into channel opening [39] have reported disease-associated GRIN2B variants in the N-terminal domain, membrane-proximal ligand-binding domain, and transmembrane domain that forms the ion pore containing three TSDs followed by an intracellular C-terminal PDZ-binding domain (CTD) of variable length. Shah et al. (2022) reported four variants, such as rs869312669 (p.T685P), rs387906636 (p.R682C), rs672601377 (p.N615I), and rs1131691702 (p.S526P), which are identified as phylogenetically conserved PTM drivers and are related to structural and functional impact. Hammond (2024) reported that ionotropic glutamate receptors (iGluRs), including NMDA and AMPA receptors, have four transmembrane domains (M1-M4) per subunit. M2 forms a re-entrant loop that shapes the ion selectivity filter and contributes to Ca² permeability and Mg2 block (for NMDARs), and M4 interacts with adjacent subunits and stabilizes the open/closed states of the channel. This suggests that disruptions in these domains can alter ion selectivity, permeability, destabilize gating transitions, and affect desensitization kinetics. Our study revealed the most pathogenic variants in ATD, S1, and TSD and none in the PDZ domain. The variant p.G96W is found in the GRIN2B ATD domain, revealing that it is involved in receptor assembly. We found 15 variants in the S1 region, 8 in the S2 domain, and 26 in the TSD. The most pathogenic variants, p.G459E and p.G459R, are located in the S1 domain, which is involved in the ligand-binding process. The two variants, p.E657G and p.G820R, are found in the TSD, which is involved in the reentrant pore-forming and transmembrane spanning process. Our analysis also revealed that the TSD harbors most variants and is the second-largest domain. Therefore, variations in this region could be deleterious, suggesting that all the multiple common variants of GRIN2B and related haplotypes are associated with an increased risk of autism.

The NMDAR intracellular CTD is variable in sequence and contains phosphorylation sites, as well as short docking motifs that bind proteins essential for receptor trafficking and function [41]. However, Sabo et al. [7] revealed that many variations found in CTD regions are not associated with risk for ASD, as determined by burden analysis, compared to controls. Similarly, we have not seen any variants in this region, indicating that selective evolutionary pressure across CTD domain variations is lower in the CTD than for TSD and Acute Behavioural Distarbance. This lack of variants in the CTD may suggest that variations in this region are less likely to contribute to ASD, providing important insights for future research.

Shah et al. [40] reported that GRIN2B hydrogen occupancy is positively associated with protein stability, and solvent-accessible surface area is positively related to globularity. The calculated stability, compactness, and the total globularity score account for the combined impact of the GRIN2B protein function. Multiple GRIN2B genetic variations are linked to gene expression, phylogenetic conservation, PTMs, and protein instability behavior in neurodevelopmental diseases [40]. The secondary structure prediction of GRIN2B and all 54 deleterious variants revealed a higher number of alpha helices that can tolerate variations compared to beta strands. Solvent accessibility of all 54 deleterious variants exhibited moderate surface exposure of a protein that serves as an active site and interacts with other molecules and ligands. Our conservation analysis revealed that all these nonsynonymous variants are found in protected areas [42]. It was also reported that highly conserved amino acids are found in physiologically active regions, and the biological activities change when these residues are replaced. Within a sequence, amino acids essential for folding, structural stability, or forming a

binding site may be more highly conserved [40]. Among the 54 selected variants, most were found in the TSD, indicating that all these variants are essential for protein folding, stability, and the formation of binding sites.

PTM is one mechanism that enables a significant functional expansion from the genome to the proteome, allowing each translated protein to act in diverse ways, at specific times, and in specific cells and tissues [43]. Our predictions revealed three variants with phosphorylation sites, including one frameshift (p.S31fs) in exon 3, located in the N-terminal ATD domain, causing premature termination of translation. The variations p.T685P located on the S1 domain and p.S882A located on the Cterminal PDZ domain indicate that these variations affect the protein's functionality. The p.S526P variant is located in the S1 domain, p.N615I is in the pore, and p.R682C and p.T685P are in the S2 domain, according to some studies. S1 and S2 form the ligand-binding domain, pore, re-entrant pore-forming, and transmembrane spanning domains, which may therefore explain the change in spatial conformation in the instability of the GRIN2B, which could be a risk factor for neurodevelopmental disorders.

Lemke et al. [44] conducted studies on two people with West syndrome and significant developmental delay, as well as one person with ID and focal epilepsy. The ID patient had a missense mutation in the extracellular glutamate-binding domain (p.Arg540His). In contrast, both West syndrome patients had missense mutations in the NR2B ion channel-forming re-entrant loop (p.Asn615Ile, p.Val618Gly).

Homology modeling is the most powerful method used to predict the tertiary structure of a protein in cases where a query protein has sequence similarity to a protein with a known atomic structure [44]. The homology modeling built for four variants, p.G459E, p.G459R, p.E657G, and p.G820R, with a pathogenicity score of >80%, indicates that these variants can affect the protein's shape. This leads to the disruption of the GRIN2B protein. An organism's PPI network serves as a framework for its signaling circuitry, which mediates the cellular response to environmental and genetic cues. Understanding this circuitry could enhance the prediction of gene function and cellular behavior in response to diverse signals [45]. The biological events controlled by PPI are crucial for predicting the function of target proteins and the drug-like properties of molecules. Studies have shown that many disordered proteins have more connections, which helps select therapeutic targets [46]. The loss or gain of hydrogen bonds, hydrophobic interactions, and salt bridges can alter the protein's structure and function [47]. Proteins bind through hydrophobic bonding, van der Waals forces, and salt bridges at specific binding domains on each protein. These domains can be small binding clefts or large surfaces, and can range from just a few peptides long to spanning hundreds of amino acids [48]. In our enrichment analysis, the GRIN2B protein interacts directly with high confidence with the neighboring functioning partners. Highconfidence genes have proteins with known functions defined for them.

In the present study, four variants, p.G459R, p.G459E, p.E657G, and p.G820R, lie within domains ligand-binding S1/S2 and transmembrane M1–M4 domains that are present in the brain transcript, which is a full-length isoform. Hence, clinical consequences like intellectual disability, epilepsy, and ASD arise from broad disruption of NMDAR signaling. These pathogenic variants are located on universal domains that affect all functional isoforms of GRIN2B. This gives confidence that their clinical impact is dictated by broad NMDA receptor dysfunction, not limited to a subset of isoforms.

GRIN2B variants can produce distinct functional effects as gain-of-function (GoF) and loss-of-function (LoF) changes in NMDA receptor activity. This functional stratification has direct therapeutic consequences. For example, patients with GoF variants

may benefit from NMDA receptor antagonists. In contrast, LoF variants might be more responsive to receptor agonists, co-agonists, or modulators that enhance receptor function. These approaches have the therapeutic potential of individualized, variant-informed interventions. The identification of GRIN2B variants has profound implications for both clinical diagnosis and the development of targeted therapies. GRIN2B, which encodes the GluN2B subunit of the NMDA receptor, plays a central role in synaptic transmission, plasticity, and neurodevelopment. The ability to detect and interpret these variants has advanced precision diagnostics, enabling earlier recognition of GRIN-related disorders and more accurate genetic counseling for families.

Beyond treatment, the study of GRIN2B variants contributes to the development of biomarkers for disease progression and treatment response. Electrophysiological assays and patient-derived neuronal models provide functional validation of variant effects, which can be translated into clinical decision-making frameworks. Moreover, such research supports the design of precision medicine trials, where therapies are tailored not only to the genetic variant but also to its biophysical effect on receptor kinetics and signaling. Overall, the growing body of GRIN2B research is bridging the gap between genetic discovery and clinical practice.

5. Conclusion

Current *in silico* analysis identifies the most deleterious variations, which reduce the loss of function of GRIN2B, leading to altered Central Nervous System development that contributes to ASD. The S1, S2, and TSD binding domains are less tolerant to variation than the CTD of GRIN2B. These studies strongly suggest that variations in this gene have deleterious effects on ASD. Among all the variations, the 13 variations, including six frameshifts from the N-terminal end, three split sites from the 5' end, and four nonsynonymous variations with a pathogenicity score >80% are more deleterious. These key variations are the focus of further analysis. These succinct findings may serve as a baseline for potential diagnostic and therapeutic approaches.

Acknowledgment

We greatly thank the Department of Atomic Energy, Mumbai, for awarding the Raja Ramanna Chair and Research Associate. We also acknowledge the University of Mysore and the Department of Genetics and Genomics for all the support provided.

Ethical Statement

This study does not contain any studies with human or animal subjects performed by any of the authors.

Conflicts of Interest

The authors declare that they have no conflicts of interest to this work.

Data Availability Statement

The data supporting the findings of this study are available upon request from the corresponding author.

Author Contribution Statement

Srushti S. Chavadapur: Methodology, Software, Validation, Formal analysis, Investigation, Resources, Data curation,

Writing – original draft, Writing – review & editing, Visualization. **Nallur B. Ramachandra:** Conceptualization, Methodology, Validation, Resources, Supervision, Project administration.

Supplementary Information

To view supplementary material for this article, please visit https://doi.org/10.47852/bonviewMEDIN52025991.

References

- [1] Ahnaou, A., Heleven, K., Biermans, R., Manyakov, N. V., & Drinkenburg, W. H. (2021). NMDARs containing NR2B subunit do not contribute to the LTP form of hippocampal plasticity: In vivo pharmacological evidence in rats. *International Journal of Molecular Sciences*, 22(16), 8672. https://doi.org/10.3390/ijms22168672
- [2] Bonsi, P., de Jaco, A., Fasano, L., & Gubellini, P. (2022). Postsynaptic autism spectrum disorder genes and synaptic dysfunction. *Neurobiology of Disease*, 162, 105564. https:// doi.org/10.1016/j.nbd.2021.105564
- [3] Selvanayagam, T., Hoang, N., Sarikaya, E., Howe, J., Russell, C., Iaboni, A., ..., & Scherer, S. W. (2025). Clinical utility of genome sequencing in autism: Illustrative examples from a genomic research study. *Journal of Medical Genetics*, 62(6), 413–421. https://doi.org/10.1136/jmg-2024-110463
- [4] Navarro, M., & Simpson, T. I. (2021). SFARI Genes and where to find them; classification modelling to identify genes associated with Autism Spectrum Disorder from RNA-seq data. bioRxiv. https://doi.org/10.1101/2021.01.29.428754
- [5] Sharma, B., Hussain, T., Khan, M. A., & Jaiswal, V. (2022). Exploring AT2R and its polymorphism in different diseases: An approach to develop AT2R as a drug target beyond hypertension. *Current Drug Targets*, 23(1), 99–113. https:// doi.org/10.2174/1389450122666210806125919
- [6] Sharma, B., Rehman, M. T., AlAjmi, M. F., Shahwan, M., Hussain, T., Jaiswal, V., & Khan, M. A. (2024). Computational investigation of the impact of potential AT₂R polymorphism on small molecule binding. *Journal of Biomolecular Structure and Dynamics*, 42(5), 2231–2241. https://doi.org/10.1080/07391102.2023.2204492
- [7] Sabo, S. L., Lahr, J. M., Offer, M., Weekes, A. L., & Sceniak, M. P. (2023). GRIN2B-related neurodevelopmental disorder: Current understanding of pathophysiological mechanisms. Frontiers in Synaptic Neuroscience, 14, 1090865. https://doi.org/10.3389/fnsyn.2022.1090865
- [8] Rangwala, S. H., Kuznetsov, A., Ananiev, V., Asztalos, A., Borodin, E., Evgeniev, V., ..., & Schneider, V. A. (2021). Accessing NCBI data using the NCBI sequence viewer and genome data viewer (GDV). *Genome Research*, 31(1), 159–169. https://doi.org/10.1101/gr.266932.120
- [9] UniProt Consortium. (2015). UniProt: A hub for protein information. *Nucleic Acids Research*, 43(D1), D204–D212. https://doi.org/10.1093/nar/gku989
- [10] Amann, V. A. (2022). Evaluation of in silico databases for the classification of genomic alterations in oncological samples. Master's Thesis, University of Split.
- [11] Li, C., Zhi, D., Wang, K., & Liu, X. (2022). MetaRNN: Differentiating rare pathogenic and rare benign missense SNVs and InDels using deep learning. *Genome Medicine*, 14(1), 115. https://doi.org/10.1186/s13073-022-01120-z
- [12] Lim, J., Malek, R., Toh, C. C., Sundram, M., Woo, S. Y., Yusoff, N. A., ..., & M-CaP Study. (2021). Prostate cancer

- in multi-ethnic Asian men: Real-world experience in the Malaysia Prostate Cancer (M-CaP) study. *Cancer Medicine*, 10(22), 8020–8028. https://doi.org/10.1002/cam4.4319
- [13] Choudhury, A., Mohammad, T., Anjum, F., Shafie, A., Singh, I. K., Abdullaev, B., ..., & Hassan, M. I. (2022). Comparative analysis of web-based programs for single amino acid substitutions in proteins. *Plos One*, *17*(5), e0267084. https://doi.org/10.1371/journal.pone.0267084
- [14] Garcia-Recio, A., Gómez-Tamayo, J. C., Reina, I., Campillo, M., Cordomí, A., & Olivella, M. (2021). TMSNP: A web server to predict pathogenesis of missense mutations in the transmembrane region of membrane proteins. *NAR Genomics and Bioinformatics*, 3(1), lqab008. https://doi.org/10.1093/nargab/lqab008
- [15] Wang, Y., & Chen, L. (2022). DeepPerVar: A multi-modal deep learning framework for functional interpretation of genetic variants in personal genome. *Bioinformatics*, 38(24), 5340–5351. https://doi.org/10.1093/bioinformatics/btac696
- [16] Poon, K. S., & Tan, K. M. L. (2022). Variant curation is crucial to claim digenic inheritance in juvenile open angle glaucoma. *Global Medical Genetics*, 9(01), 054–055. https://doi.org/10. 1055/s-0041-1733963
- [17] Ashrafzadeh, S., Golding, G. B., Ilie, S., & Ilie, L. (2024). Scoring alignments by embedding vector similarity. *Briefings in Bioinformatics*, 25(3), bbae178. https://doi.org/10.1093/bib/bbae178
- [18] Kuksa, P. P., Greenfest-Allen, E., Cifello, J., Ionita, M., Wang, H., Nicaretta, H., ..., & Leung, Y. Y. (2022). Scalable approaches for functional analyses of whole-genome sequencing non-coding variants. *Human Molecular Genetics*, 31(R1), R62–R72. https://doi.org/10.1093/hmg/ddac191
- [19] Bashar, M. A., Barua, L., Paul, S., Dash, N., Sadhu, T., Mitra, S., & Dash, R. (2024). Elucidating conformational alteration of human islet amyloid polypeptide by nonsynonymous substitution. bioRxiv, 2024-11. https://doi.org/10.1101/2024. 11.16.623924.
- [20] Ahmad, R. M., Ali, B. R., Al-Jasmi, F., Al Dhaheri, N., Al Turki, S., Kizhakkedath, P., & Mohamad, M. S. (2024). Al-derived comparative assessment of the performance of pathogenicity prediction tools on missense variants of breast cancer genes. *Human Genomics*, 18(1), 99. https://doi.org/10.1186/s40246-024-00667-9.
- [21] Qi, H., Zhang, H., Zhao, Y., Chen, C., Long, J. J., Chung, W. K., ..., & Shen, Y. (2021). MVP predicts the pathogenicity of missense variants by deep learning. *Nature Communications*, 12(1), 510. https://doi.org/10.1038/s41467-020-20847-0
- [22] Zhang, H., Xu, M. S., Fan, X., Chung, W. K., & Shen, Y. (2022). Predicting functional effect of missense variants using graph attention neural networks. *Nature Machine Intelligence*, 4(11), 1017–1028. https://doi.org/10.1038/s42256-022-00561-w
- [23] Pejaver, V., Urresti, J., Lugo-Martinez, J., Pagel, K. A., Lin, G. N., Nam, H. J., ..., & Radivojac, P. (2020). Inferring the molecular and phenotypic impact of amino acid variants with MutPred2. *Nature Communications*, 11(1), 5918. https://doi.org/10.1038/s41467-020-19669-x
- [24] Steinhaus, R., Proft, S., Schuelke, M., Cooper, D. N., Schwarz, J. M., & Seelow, D. (2021). MutationTaster2021. Nucleic Acids Research, 49(W1), W446–W451. https://doi.org/10.1093/nar/ gkab266
- [25] Malhis, N., Jacobson, M., Jones, S. J., & Gsponer, J. (2020).
 LIST-S2: Taxonomy based sorting of deleterious missense

- mutations across species. *Nucleic Acids Research*, 48(W1), W154–W161. https://doi.org/10.1093/nar/gkaa288
- [26] Shakibaie, M. R. (2021). In silico characterization of biofilm-associated protein (Bap) identified in a multi-drug resistant Acinetobacter baumannii clinical isolate. Journal of Medical Microbiology and Infectious Diseases, 9(4), 210–220. https://doi.org/10.52547/JoMMID.9.4.210
- [27] Janaki, C., Gowri, V. S., & Srinivasan, N. (2021). Master Blaster: An approach to sensitive identification of remotely related proteins. *Scientific Reports*, 11(1), 8746. https://doi. org/10.1038/s41598-021-87833-4
- [28] Yang, J., & Zhang, Y. (2015). Protein structure and function prediction using I-TASSER. Current Protocols in Bioinformatics, 52(1), 5–8. https://doi.org/10.1002/ 0471250953.bi0508s52
- [29] Yariv, B., Yariv, E., Kessel, A., Masrati, G., Chorin, A. B., Martz, E., ..., & Ben-Tal, N. (2023). Using evolutionary data to make sense of macromolecules with a "face-lifted" ConSurf. *Protein Science*, 32(3), e4582. https://doi.org/10. 1002/pro.4582
- [30] Wang, D., Liu, D., Yuchi, J., He, F., Jiang, Y., Cai, S., ..., & Xu, D. (2020). MusiteDeep: A deep-learning based webserver for protein post-translational modification site prediction and visualization. *Nucleic Acids Research*, 48(W1), W140–W146. https://doi.org/10.1093/nar/gkaa275
- [31] Madsen, C. D., Hein, J., & Workman, C. T. (2022). Systematic inference of indirect transcriptional regulation by protein kinases and phosphatases. *PLoS Computational Biology*, 18(6), e1009414. https://doi.org/10.1371/journal.pcbi.1009414
- [32] Paritala, V. E. N. U. (2022). Comparative modeling for *Saccharomyces cerevisiae* RAD56 using Swiss-model, I-Tasser, and Phyre2. *International Journal of Pharmaceutics*, *14*(4), 28–33. https://doi.org/10.22159/ijpps.2022v14i4.43972
- [33] Jejurikar, B. L., & Rohane, S. H. (2021). Drug designing in Discovery Studio. *Asian Journal of Research in Chemistry*, 14(2), 135–138.
- [34] Szklarczyk, D., Nastou, K., Koutrouli, M., Kirsch, R., Mehryary, F., Hachilif, R., ..., & von Mering, C. (2025). The STRING database in 2025: Protein networks with directionality of regulation. *Nucleic Acids Research*, *53*(D1), D730–D737. https://doi.org/10.1093/nar/gkae1113
- [35] Pruitt, K. D., Tatusova, T., & Maglott, D. R. (2007). NCBI reference sequences (RefSeq): A curated non-redundant sequence database of genomes, transcripts and proteins. *Nucleic Acids Research*, *35*(suppl_1), D61–D65. https://doi.org/10.1093/nar/gkl842
- [36] Mangano, G. D., Riva, A., Fontana, A., Salpietro, V., Mangano, G. R., Nobile, G., ..., & Nardello, R. (2022). De novo GRIN₂A variants associated with epilepsy and autism and literature review. *Epilepsy & Behavior*, 129, 108604. https://doi.org/10.1016/j.yebeh.2022.108604
- [37] Jiang, W., & Chen, L. (2021). Alternative splicing: Human disease and quantitative analysis from high-throughput sequencing. *Computational and Structural Biotechnology Journal*, 19, 183–195. https://doi.org/10.1016/j.csbj.2020.12.009

- [38] Adorno-Farias, D., Santos, J. N. D., González-Arriagada, W., Tarquinio, S., Santibanez Palominos, R. A., Martin, A. J., & Fernandez-Ramires, R. (2023). Whole-exome sequencing of oral epithelial dysplasia samples reveals an association with new genes. *Brazilian Oral Research*, 37, e016. https://doi.org/10.1590/1807-3107bor-2023.vol37.0016
- [39] Stroebel, D., & Paoletti, P. (2021). Architecture and function of NMDA receptors: An evolutionary perspective. *The Journal of Physiology*, 599(10), 2615–2638. https://doi.org/10.1113/ JP279028
- [40] Shah, A. A., Amjad, M., Hassan, J. U., Ullah, A., Mahmood, A., Deng, H., ..., & Xia, K. (2022). Molecular insights into the role of pathogenic nsSNPs in *GRIN2B* gene provoking neurodevelopmental disorders. *Genes*, 13(8), 1332. https://doi.org/10.3390/genes13081332
- [41] Hammond, C. (2024). The ionotropic glutamate receptors. In *Cellular and Molecular Neurophysiology*, 221–244.
- [42] Zhou, M. H., Chen, S. R., Wang, L., Huang, Y., Deng, M., Zhang, J., ..., & Pan, H. L. (2021). Protein kinase C-mediated phosphorylation and α2δ-1 interdependently regulate NMDA receptor trafficking and activity. *Journal of Neuroscience*, 41(30), 6415–6429. https://doi.org/10.1523/ JNEUROSCI.0757-21.2021
- [43] Adoni, K. R., Cunningham, D. L., Heath, J. K., & Leney, A. C. (2022). FAIMS enhances the detection of PTM crosstalk sites. *Journal of Proteome Research*, 21(4), 930–939. https://doi.org/ 10.1021/acs.jproteome.1c00721
- [44] Lemke, G. (2001). Glial control of neuronal development. *Annual Review of Neuroscience*, 24(1), 87–105. https://doi.org/0147-006X/01/0301-0087\$14.00
- [45] Agnihotry, S., Pathak, R. K., Singh, D. B., Tiwari, A., & Hussain, I. (2022). Protein structure prediction. In *Bioinformatics* (pp. 177–188). Academic Press.
- [46] Martini, L., Baek, S. H., Lo, I., Raby, B. A., Silverman, E. K., Weiss, S. T., ..., & Halu, A. (2024). Detecting and dissecting signaling crosstalk via the multilayer network integration of signaling and regulatory interactions. *Nucleic Acids Research*, 52(1), e5. https://doi.org/10.1093/nar/gkad1035
- [47] Ahmad, S. U., Ali, Y., Jan, Z., Rasheed, S., Nazir, N. U. A., Khan, A., ..., & Rehman, A. U. (2023). Computational screening and analysis of deleterious nsSNPs in human p14ARF (CDKN2A gene) protein using molecular dynamic simulation approach. Journal of Biomolecular Structure and Dynamics, 41(9), 3964–3975. https://doi.org/10.1080/07391102.2022.2059570
- [48] Cao, L., Coventry, B., Goreshnik, I., Huang, B., Sheffler, W., Park, J. S., ..., & Baker, D. (2022). Design of protein-binding proteins from the target structure alone. *Nature*, 605(7910), 551–560. https://doi.org/10.1038/s41586-022-04654-9

How to Cite: Chavadapur, S. S., & Ramachandra, N. B. (2025). Computational Genomic Variations of GRIN2B Associated with Autism Spectrum Disorders: An *In Silico* Approach. *Medinformatics*. https://doi.org/10.47852/bonviewMEDIN52025991